THE ZEEMAN EFFECT IN THE ORTHO-HELIUM BAND SPECTRUM

By John S. Millis
Ryerson Physical Laboratory, University of Chicago

(Received July 16, 1931)

Abstract

Resolved and partially resolved Zeeman patterns have been obtained at high dispersion for ortho-helium bands of the types $nd\delta,{}^3\Delta\rightarrow 2p\pi,{}^3\Pi$; $nd\pi,{}^3\Pi\rightarrow 2p\pi,{}^3\Pi$; and $nd\sigma,{}^3\Sigma\rightarrow 2p\pi,{}^3\Pi$. For small values of rotational energy, these patterns agree with the theoretical predictions for a case b' molecule. Departure from these predictions, which increases with n, K, and $l-\lambda$, is noted in all of the above bands. Patterns of some levels of large rotational energy approximate the predctions for a case d' molecule. This departure is in agreement with predictions and observations of the energy changes incident to the uncoupling of the orbital angular momentum of the excited electron from the molecular axis. Thus, the Zeeman effect affords a method of tracing the progress of this uncoupling phenomenon. Evidence is given that the line $Q(9)$ of the band $4p\pi,{}^3\Pi^{(0)}\rightarrow 2s\sigma,{}^3\Sigma^{(0)}$ has a triplet structure without field.

Introduction

Theoretical Expectations

A NUMBER of authors[1] have discussed the energy changes occurring in a molecule when the coupling of the electronic orbital angular momentum to the electric axis is varied. They have pointed out that marked energy changes should occur in light molecules when this coupling is changed from the condition of rigid coupling to that of partial or total uncoupling. It has been further pointed out that such uncoupling of the angular momentum should be most pronounced for large values of the total quantum number, n, of the excited electron, for large values of the rotational quantum number, K, and should become more obvious with increasing difference between the orbitual angular momentum quantum number, l, of the excited electron, and its projection on the electric axis, λ. Several investigators[2] have reported evidence of uncoupling phenomena in accordance with these predictions in the ortho-helium band spectrum, which is theoretically a triplet spectrum ($S=1$), and also in the parhelium spectrum ($S=0$).

If the coupling in the helium molecule is rigid, the orbital angular momentum of the excited electron is so coupled to the electric axis that its projection thereon, λ, is a true quantum number.[3] Mulliken and Monk[4] have shown that the triplet structure in the ortho-helium bands is detectable only

[1] Cf. W. E. Curtis, Trans. Faraday Soc. **25**, 694 (1929), for full references.

[2] W. Weizel, Zeits. f. Physik **52**, 175 (1928), and G. H. Dieke, Zeits. f. Physik **57**, 71 (1929).

[3] Cf. R. S. Mulliken, Reviews of Modern Physics **2**, 97 et seq., Jan., 1930 and **2**, 506, Sept., 1930 for a complete discussion.

[4] R. S. Mulliken and G. S. Monk, Phys. Rev. **34**, 1530 (1929).

in the $2p\pi$, $^3\Pi$ state and that even this structure disappears in a weak magnetic field (i.e., the Paschen-Back effect becomes total at a low value of the magnetic field). Hence the bands in a strong magnetic field may be treated as if they were singlet bands. This case of triplet bands which behave like singlet bands has been classified under case b'.[3] The energy of a case b' singlet state in a magnetic field of strength H is well known to be [5,6]

$$\Delta E_{\text{mag}} = \frac{\mu_1 H M \Lambda^2}{K(K+1)} \tag{1}$$

where M is the magnetic quantum number, K the rotational quantum number, $\Lambda = \lambda$ for the present case, and $\mu_1 = eh/4\pi mc$. Curtis and Jevons[7] and Mulliken and Monk[4] have reported observations upon the Zeeman effect in some $s\sigma$, $^3\Sigma \rightarrow 2p\pi$, $^3\Pi$ ortho-helium bands. The resolved patterns are in agreement with the case b' predictions and the widths of the unresolved lines seem also to conform to case b' expectations.

If, the electronic angular momentum becomes completely uncoupled from the electric axis, the molecule conforms to Hund's case d'.[3] The same argument as advanced above holds, so that the structure may be considered to be that of a singlet state. The energy of a case d' state in a magnetic field can be easily calculated in a manner similar to that used in deriving relation (1). This leads to the expression[6]

$$\Delta E_{\text{mag}} = \frac{\mu_1 H M}{2K(K+1)}[K(K+1) + L(L+1) - R(R+1)] \tag{2}$$

where R is the nuclear rotation quantum number, L the orbital angular momentum quantum number (l for the present case), and K is the quantized resultant of L and R.

In general the magnetic energies of the two above cases are considerably different, the case d' energy being usually greater than that of case b'. Obviously, therefore, the Zeeman effect should afford a method of determining the degree of conformity to the two cases. Since complete uncoupling is not expected to occur at any critical value of n, K, or l-λ, many levels will correspond to cases intermediate between case b' and case d'. Hence the width of the Zeeman patterns should indicate, at least qualitatively, the degree of uncoupling. Harvey[8] has reported the qualitative effect of a magnetic field upon the orthohelium band lines involving levels of the $nd\delta$,$^3\Delta$; $nd\pi$,$^3\Pi$; $nd\sigma$,$^3\Sigma$ types. The extreme broadening of these lines led him to conclude that there is evidence of uncoupling in all of these levels.

Inasmuch as the Zeeman patterns of all but the first lines of the various branches of a band consist of a large number of components, a great number of them appear unresolved even at high dispersion. However, intensity re-

[5] F. Hund, Zeits. f. Physik **36,** 657 (1926).
[6] Cf. appendix for derivation of this and relation (2) given below.
[7] W. E. Curtis and W. Jevons, Proc. Roy. Soc. **A120,** 110 (1928).
[8] A. Harvey, Proc. Roy. Soc. **A126** ,583 (1930).

lations aid in comparing predicted overall widths with observations. Hönl[9] and Kronig[10] have given formulas which predict the relative intensities I, of the components of a spectral line in a magnetic field. These formulas apply equally well to case b' and case d' and may be stated as follows:

For Q branches,

$$M' = M'' + 1, \quad I = (\tfrac{1}{4})(K' - M' + 1)(K' + M')$$
$$M' = M'', \quad I = M'^2$$
$$M' = M'' - 1, \quad I = (\tfrac{1}{4})(K' - M')(K' + M' + 1)$$

For R branches,

$$M' = M'' + 1, \quad I = (\tfrac{1}{4})(K' + M' - 1)(K' + M')$$
$$M' = M'', \quad I = K'^2 - M'^2$$
$$M' = M'' - 1, \quad I = (\tfrac{1}{4})(K' - M' - 1)(K' - M')$$

For P branches,

$$M' = M'' + 1, \quad I = (\tfrac{1}{4})(K' - M' + 1)(K' - M' + 2)$$
$$M' = M'', \quad I = (K' + 1)^2 - M'^2$$
$$M' = M'' - 1, \quad I = (\tfrac{1}{4})(K' + M' + 1)(K' + M' + 2)$$

To check the predictions described above in a more quantitative manner than has been done by previous investigators, a fairly extensive investigation of the Zeeman effect in the ortho-helium bands under high dispersion was carried out.

Experimental Procedure

The helium discharge tube used in this investigation was of a special form designed by Mr. L. E. Pinney and fully described by Mulliken and Monk.[4] It consists of a Pyrex tube shaped to fit in the pole gap of a water-cooled magnet. The bands were excited by a small current from the secondary of a $\frac{1}{2}$ K.V.A. transformer with the usual spark gap in series. With a pressure of approximately 3 cm of helium in the tube the bands appeared with fair intensity. The discharge took place between the overlapping tips of a pair of aluminum electrodes placed normal to the magnetic field. The total discharge was confined to the center of the field and thus all radiation came from a uniform field. With the tubes used, giving a pole gap of about 6 mm, and a current of 12 amperes in the field windings, fields of from 28,000 to 30,500 gauss were obtained. The field strength of each plate was determined from the splitting of the atomic helium lines which were conveniently present.

The spectrum was photographed in the second and third orders of a twenty-one foot concave grating in a Rowland mounting, which gave a dispersion of 1.31A per mm in the second order. A large Nicol prism was placed in front of the spectrograph slit so that on all photographs only one polarization

[9] H. Hönl, Zeits. f. Physik **31**, 340 (1926).
[10] R. De L. Kronig, Zeits. f. Physik **31**, 885 (1926).

appeared. With the system used, the spectrum was of very low intensity so that exposures of from three to five days were necessary. An iron comparison spectrum was used on each plate.

Comparison of Experiment with Theory

The observed results are given in detail in the central column of the appended table. Tabulated on each side of the observations are the predicted results for case b' and for case d'. The component of each line which according to theory should appear with the maximum intensity is underlined. All of the separations are in terms of $\Delta\nu_{\text{normal}}$[11], i.e., half the width of the normal atomic triplet. The vast majority of the lines become, in the magnetic field, very diffuse so that comparator measurements of the overall widths of Zeeman patterns are not very reliable. However, microphotometer traces of the band lines indicate the degree of reliability of the various measurements. In the table the following notation has been used- s for singlet, d for doublet, t for triplet, q for quartet, (i.e., lines for which microphotometer traces indicate 1, 2, 3, or 4 maxima) and b for broad, for which traces give a wide maximum of fairly steep sides so that an overall width may be determined. Obviously the measurements marked d, t, or q are fairly reliable while those marked b are considerably less so.

Portions of typical bands are shown diagrammatically in Fig. 1 and 3. The predicted patterns have been drawn to scale both as to separation and relative intensity for each polarization. The photometer traces of the individual lines have been cut out and pasted on the diagrams between the predicted patterns. The scale of the traces varies, not only with the wave-length, but also for lines of nearly the same wave-length, since traces of both second and third order photographs were used. Since the traces have been used without enlargement or reduction, the scales of the predicted and observed patterns in the figures are often quite different, those of the predicted patterns being usually greater. This should be borne in mind when one examines the figures. The numbers below each predicted and observed pattern, however, expresses the indicated widths in terms of $\Delta\nu_{\text{normal}}$. In some cases the trace was not of sufficient density to photograph well so that it has been inked over. The trace of the line $Q(3)$ of $3d\sigma,{}^3\Sigma^{(0)}\rightarrow 2p\pi,{}^3\Pi^{(0)}$ in perpendicular polarization has been partially reconstructed since it is slightly overlapped by another line.

The comparison of prediction and observation can be made quite easily from an inspection of the figures and the table, but a brief account of its results will be given.

In the Q branch of the band $3p\pi,{}^3\Pi^{(0)}\rightarrow 2s\sigma,{}^3\Sigma^{(0)}$ nothing can be deduced concerning the conformity to the limiting cases b' and d', since the predicted patterns are identical. The agreement, however, with these predictions is obviously good. The measurements on the R branch of this band agree reasonably well with case b' predictions. The doublet structure decreases in width for increasing values of K in perpendicular polarization. The parallel

[11] $\Delta\nu_{\text{normal}}$ on the plates obtained corresponded at a wave-length of 4471A to a separation of 0.392 mm or 2.415 cm^{-1} for a field of 30,000 gauss.

polarization measurements in this branch also check well with case b' expectations. The excellent agreement for the line $R(1)$ as indicated in Fig. 1 is

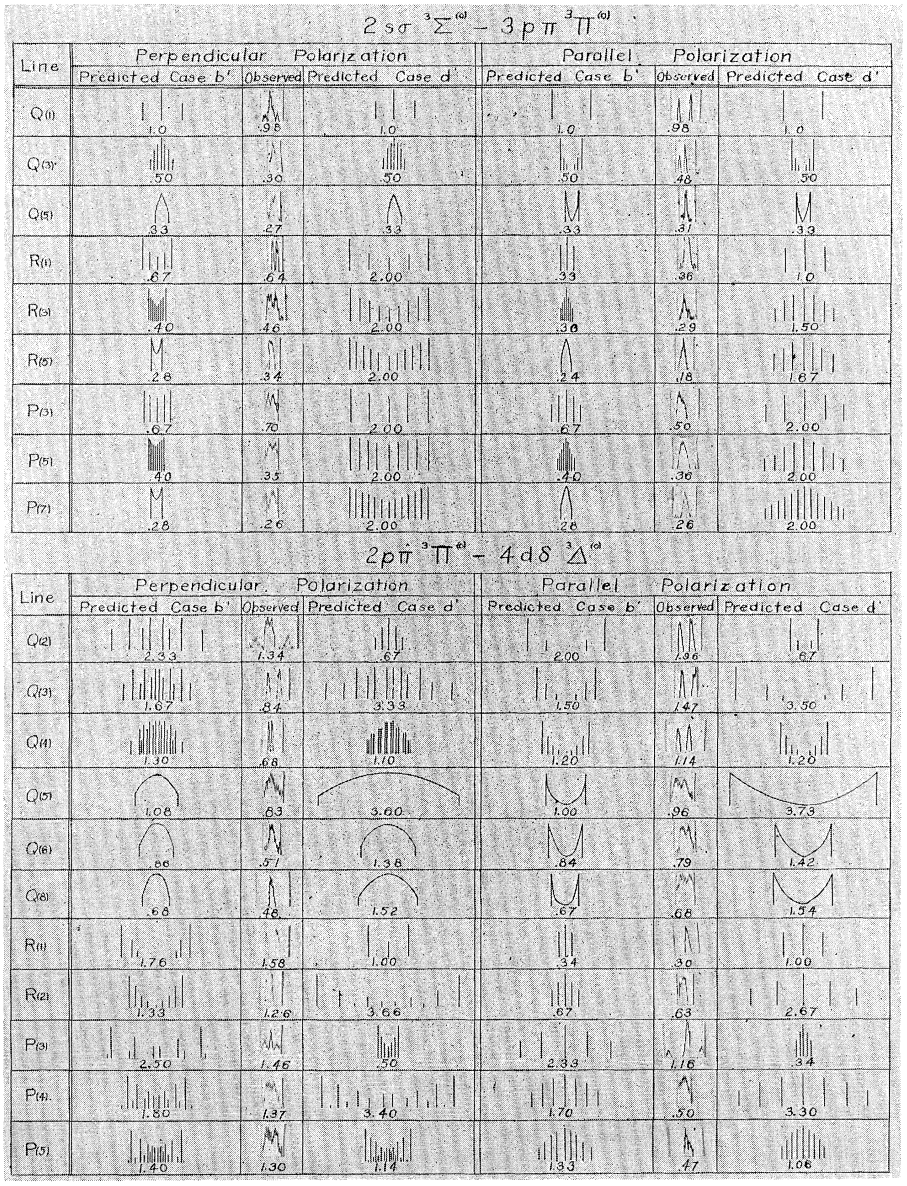

Fig. 1. Comparison of predicted Zeeman patterns and microphotometer traces of observed lines in bands in which there is little or no evidence of uncoupling phenomena The scale of the observed patterns is not uniform and is not the same as that of the predicted patterns.

of interest. The P branch also follows case b' predictions, although no resolved patterns were obtained.

The band $4p\pi,{}^3\Pi^{(0)}\rightarrow 2s\sigma,{}^3\Sigma^{(0)}$ gives patterns almost identical with those appearing in the corresponding lines in the band just discussed. The line $Q(9)$ is however anomalous. Curtis and Jevons[7] have described this line as a doublet of separation 6.6 cm^{-1} on zero-field plates. They further report that both components appear very broad in a magnetic field, the short-wave component ($\lambda = 3681.29$) being made so broad and diffuse as to nearly disappear. Although the band has not been observed without field by the author, it has been measured at field strengths of 5,000 gauss, and of 30,400 gauss in both polarizations. On all three plates it appears as a distinct and asymmetrical triplet with the long-wave and short-wave components separated from the central component by 1.61 cm^{-1} and 5.80 cm^{-1} respectively. This corresponds to a separation between the short-wave component and the center of gravity of the two long-wave components of 6.61 cm^{-1}. The three components are of

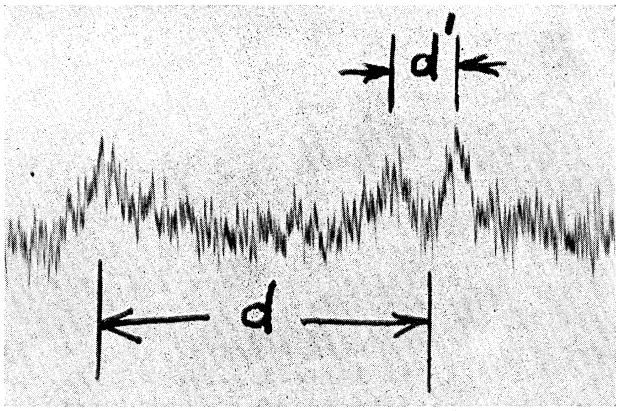

Fig. 2. Microphotometer trace of the anomalous line $Q(9)$ of $4p\pi,{}^3\Pi^{(0)}-2s\sigma,{}^3\Sigma^{(0)}$ in a magnetic field of 30,400 gauss. The perpendicular polarization is here reproduced but the trace in parallel polarization is very nearly identical. $d = 6.61$ cm^{-1}, $d' = 1.61$ cm^{-1}.

about equal intensity. On the high field plates all of these lines are considerably broadened, the width decreasing for the three components with increasing wave-length. The widths observed are about the same as those expected for the $Q(9)$ line if it were single. The observed structure is apparently identical with that observed by Curtis and Jevons for the line $Q(9)$ in the 1,1 band. A probable interpretation of this structure is that a perturbation here occurs which causes the molecule to behave as in case b or case a instead of as in case b'. The line is no doubt a triplet both with and without field, corresponding to $K = 9$, $J = 8$, 9, and 10.[12] The microphotometer trace of this line is reproduced in Fig. 2.

The lines $Q(9)$ of the 0,1 and 1,1 bands of the same system look like doublets but are so faint that no measurements could be made, while the micro-

[12] Cf. G. H. Dieke, Nature, March 23, 1929 and R. S. Mulliken and G. S. Monk, Phys. Rev. **34**, 1532 (1929).

photometer traces are complicated by large plate grain. This is in agreement with the observations of Curtis and Jevons, save that no splitting has been bound in the long-wave component of the line in the 1,1 band, possibly due to the extreme faintness. This band system also shows perturbations in the lines $R(5)$ and $P(7)$. No resolved patterns appear, but both of these lines in the 0,0 band are wider on the author's plates than their neighbors, i.e., $R(3)$, $R(7)$ and $P(5)$, $P(9)$ respectively.

The band $4s\sigma,^3\Sigma^{(0)}\rightarrow 2p\pi,^3\Pi^{(0)}$ exhibits Zeeman effects in close agreement with case b' predictions. The agreements for the three bands so far discussed are in accordance with the reports of previous investigators. It is, therefore, safe to conclude that there is very little uncoupling of the orbital angular momentum in the $np\pi\ ^3\Pi$ levels. Since the level $2p\pi$, $^3\Pi$ is the final state in all other bands studied here, it has been assumed that any uncoupling phenomenon which may occur must be a property of the initial state only.

In the band $4d\delta,^3\Delta^{(0)}\rightarrow 2p\pi,^3\Pi^{(0)}$ predictions for both case b' and case d' give very large patterns for small rotational energies. It is therefore dangerous to draw conclusions from unresolved patterns. However, inspection of Fig. 1 does reveal that the lines $Q(2)$, $R(1)$, $R(2)$, $P(3)$, $P(4)$, $P(5)$ in the perpendicular polarization and $Q(2)$, $Q(3)$, $Q(5)$, $Q(6)$, $Q(8)$, and $P(3)$ in the parallel polarization give evidence in favor of case b' coupling for the values of K involved. For large values of K a departure from case b' appears in the lines $Q(10)$, $P(9)$, $Q(14)$, and $P(11)$. However in none of these does the pattern conform at all closely to a case d' prediction. The failure to observe weak components which should appear at the edge of several lines in this band and others is probably due to the large grain of the rapid plates used. Microphotometer traces of such components are completely masked by the variations in density due to this grain. The evidence furnished by the band $3d\delta$, $^3\Delta^{(0)}\rightarrow 2p\pi,^3\Pi^{(0)}$ is identical. Conformity to case b' for low values of rotational energy is shown as above, but no lines involving large values of K were observed so that departure from this case is not shown. One may conclude that, in the levels $4d\delta,^3\Delta$ and $3d\delta,^3\Delta$, coupling of the orbital angular momentum of the excited electron to the electric axis is strong for all values of K less than nine and becomes weakened for large values of the rotation, though this uncoupling proceeds slowly. It should be pointed out that this is not in perfect agreement with the conclusions of Harvey[8] for these states. He concluded that the great width of lines in the field corresponding to small K values was indicative of uncoupling. A brief inspection of Figure 1 shows that case b' predictions are wider than case d' predictions for very small rotational energies. It is obvious, therefore, that great width of pattern alone is not indicative of the presence of uncoupling phenomona.

In the band $4d\pi,^3\Pi^{(0)}\rightarrow 2p\pi,^3\Pi^{(0)}$ the evidence of uncoupling occurs at much smaller rotational energies than in the last cases discussed above. The level $K=2$ is very apparently a case b' state as shown in the resolved patterns of the lines $Q(2)$ and $P(3)$ illustrated in Fig. 3. But for all values of K greater than two, there is departure from case b' predictions which increases with K so that for the line $R(15)$ the width of the pattern approaches fairly closely

the width of the case d' prediction. Similar evidence is offered by the band $3d\pi,{}^3\Pi^{(0)}\rightarrow 2p\pi,{}^3\Pi^{(0)}$. However it should be noted that the departure from

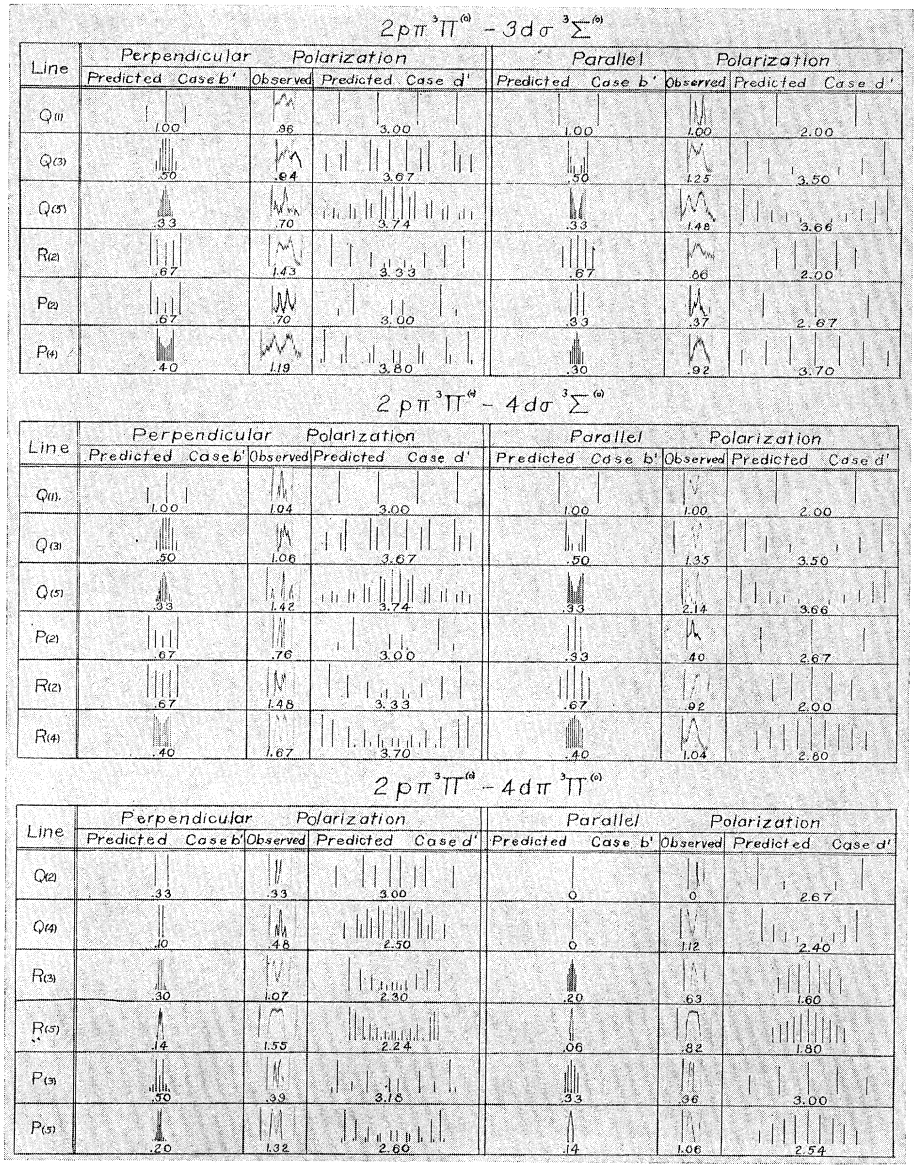

Fig. 3. Comparison of predicted and observed Zeeman patterns in bands which exhibit considerable evidence of uncoupling phenomena. The scales of the observed and predicted patterns are not the same.

case b' is less for the lines of this band than for the corresponding members of the band involving $4d\pi,{}^3\Pi$.

The uncoupling phenomenon appears for small values of K also in the band $3d\sigma,{}^3\Sigma^{(0)'}\rightarrow 2p\pi,{}^3\Pi^{(0)}$. For $K=1$, the agreement between observation and case b' predictions is excellent as is evident in Fig. 3 for the resolved patterns of the lines $Q(1)$ and $P(2)$. But for all larger values of K the observations depart from case b' and this departure increases rapidly with increasing K. The

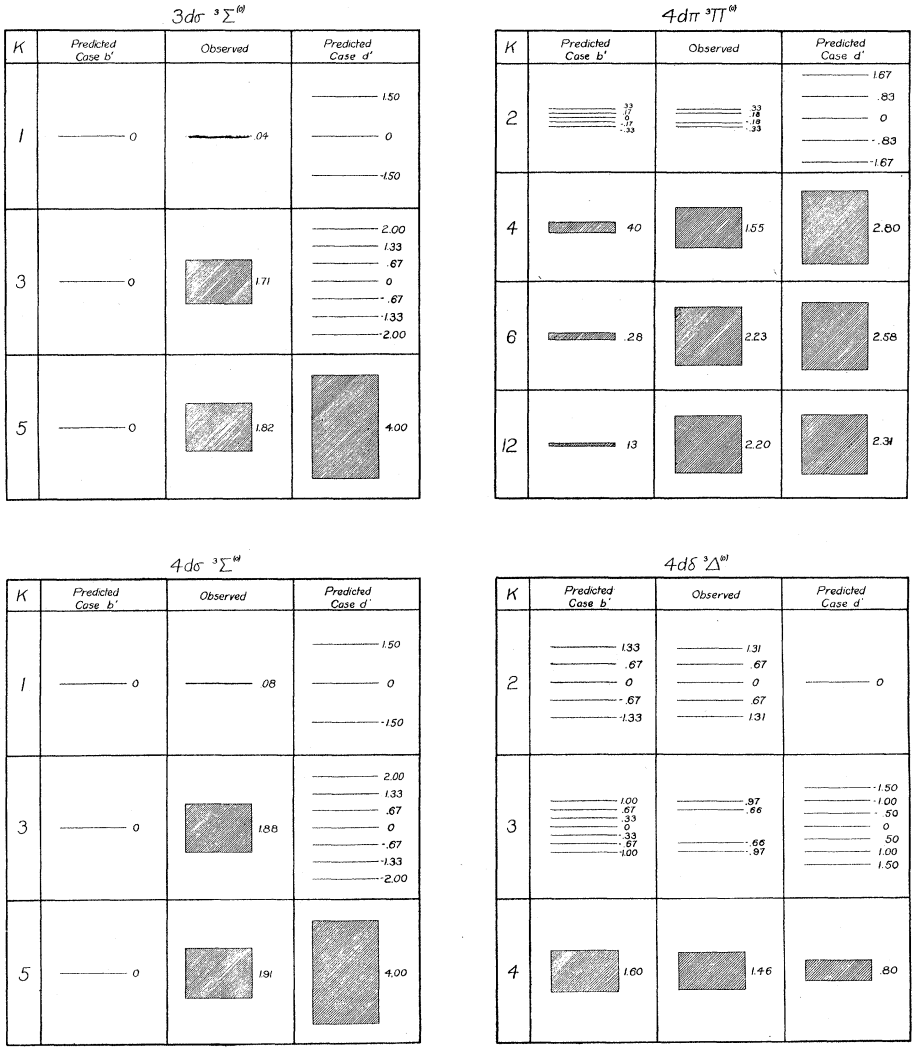

Fig. 4. Magnetic field energy level patterns for some states exhibiting uncoupling phenomena.

rate of departure is more rapid than for the bands involving $nd\pi,{}^3\Pi$ levels. The band $4d\sigma,{}^3\Sigma^{(0)}\rightarrow 2p\pi,{}^3\Pi^{(0)}$ furnishes exactly similar evidence. The patterns for this band are slightly wider than those of corresponding lines in $3d\sigma,{}^3\Sigma^{(0)}\rightarrow 2p\pi,{}^3\Pi^{(0)}$, indicating more rapid uncoupling, as can be easily seen in Fig. 3.

TABLE I.

The following notation has been used to describe the observed results: s, singlet; d, doublet, t, triplet; q, quartet; b, broad. All separations of components in resolved patterns and widths of unresolved patterns are expressed in terms of $\Delta\nu_{\text{normal}}$. This corresponds at $\lambda=4471$, to a separation of 0.392 mm or 2.415 cm^{-1} for a field of 30,000 gauss. The component of the predicted patterns which is expected to appear with maximum intensity is overscored.

Line	Predicted, Case b'	Observed	Predicted, Case d'
	$3p\pi,{}^3\Pi^{(0)}\rightarrow 2s\sigma,{}^3\Sigma^{(0)}$ ($\lambda=4675$)		
$Q(1)$	(σ) $\pm.50,\overline{0}$	t $\pm.49,0$	$\pm.50,\overline{0}$
	(π) $\pm.50$	d .98	$\pm.50$
$Q(3)$	(σ) $\pm.25,.17,.08,\overline{0}$	b .30	$\pm.25,.17,.08,\overline{0}$
	(π) $\pm.\overline{25},.17,.08$	d .48	$\pm.\overline{25},.17,.08$
$Q(5)$	(σ) $\pm.17,.13,.10,.07,.03,\overline{0}$	b .27	$\pm.17,.13,.10,.07,.03,\overline{0}$
	(π) $\pm.\overline{17},.13,.10,.07,.03$	d .31	$\pm.\overline{17},.13,.10,.07,.03$
$Q(7)$	(σ) overall .25	b .25	overall .25
	(π) overall .25	d .20	overall .25
$Q(9)$	(π) overall .20	d .20	overall .20
$Q(11)$	(π) overall .17	d .16	overall .17
$R(1)$	(σ) $\pm.\overline{33},.17,0$	d .64	$\pm\overline{1}.\overline{00},.50,0$
	(π) $\pm.17,\overline{0}$	t $\pm.16,0$	$\pm.50,\overline{0}$
$R(3)$	(σ) $\pm.\overline{20},.15,.10,.05,0$	d .46	$\pm\overline{1}.\overline{00},.75,.50,.25,\overline{0}$
	(π) $\pm.15,.10,.05,\overline{0}$	b .29	$\pm.75,.50,.25,\overline{0}$
$R(5)$	(σ) overall .28	d .34	overall 2.00
	(π) overall .24	b .18	overall 1.67
$R(7)$	(σ) overall .22	d .21	overall 2.00
	(π) overall .19	b .16	overall 1.75
$R(9)$	(σ) overall .18	d .17	overall 2.00
	(π) overall .16	s	overall 1.80
$P(3)$	(σ) $\pm.33,.17,0$	d .70	$\pm\overline{1}.\overline{00},.50,0$
	(π) $\pm.33,.17,\overline{0}$	b .50	$\pm1.00,.50,\overline{0}$
$P(5)$	(σ) $\pm.\overline{20},.15,.10,.05,0$	d .35	$\pm\overline{1}.\overline{00},.75,.50,.25,0$
	(π) $\pm.20,.15,.10,.05,\overline{0}$	b .36	$\pm1.00,.75,.50,.25,\overline{0}$
$P(7)$	(σ) overall .25	d .26	overall 2.00
	(π) overall .25	b .26	overall 2.00
	$4p\pi,{}^3\Pi^{(0)}\rightarrow 2s\sigma,{}^3\Sigma^{(0)}$ ($\lambda=3676$)		
$Q(1)$	(σ) $\pm.50,\overline{0}$	t $\pm.50,0$	$\pm.50,\overline{0}$
	(π) $\pm.50$	d 1.07	$\pm.\overline{50}$
$Q(3)$	(σ) $\pm.25,.17,.08,\overline{0}$	b .31	$\pm.25,.17,.08,\overline{0}$
	(π) $\pm.\overline{25},.17,.08$	d .51	$\pm.25,.17,.08$
$Q(5)$	(σ) $\pm.17,.13,.10,.07,.03,0$	b .26	$\pm.17,.13,.10,.07,.03,0$
	(π) $\pm.\overline{17},.13,.10,.07,.03$	d .33	$\pm.\overline{17},.13,.10,.07,.03$
$Q(7)$	(σ) overall .25	b .23	overall .25
	(π) overall .25	d .27	overall .25
$Q(9)$	(σ) overall .20	*	overall .20
	(π) overall .20	*	overall .20

* This line is apparently a triplet both with or without field. The three components are all broadened in the field having a width of approximately .20 in both polarizations. See text for full description and discussion.

TABLE I. (*Continued*)

Line	Predicted, Case b'	Observed		Predicted, Case d'
$R(1)$	(σ) $\pm .\overline{33}, .17, 0$	d	.67	$\pm\overline{1}.\overline{00}, .50, 0$
$R(3)$	(σ) $\pm .\overline{20}, .15, .10, .05, 0$	d	.39	$\pm\overline{1}.\overline{00}, .75, .50, .25, 0$
$R(5)$	(σ) overall .29	d	.41	overall 2.00
$R(7)$	(σ) overall .22 (π) overall .19	d s	.25	overall 2.00 overall 1.80
$R(9)$	(σ) overall .18 (π) overall .16	d s	.23	overall 2.00 overall 1.80
$P(3)$	(σ) $\pm .\overline{33}, .17, 0$	d	.65	$\pm\overline{1}.\overline{00}, .50, 0$
$P(5)$	(σ) $\pm .\overline{20}, .15, .10, .05, \overline{0}$	d	.66	$\pm\overline{1}.\overline{00}, .75, .50, .25, \overline{0}$
$P(7)$	(σ) overall .29	d	.28	overall 2.00
	$4s\sigma, {}^3\Sigma^{(0)} \rightarrow 2p\pi, {}^3\Pi^{(0)}$ ($\lambda = 4545$)			
$Q(1)$	(σ) $\pm .50, \overline{0}$ (π) $\pm .\overline{50}$	t d	$\pm .49, 0$ .96	
$Q(3)$	(σ) $\pm .25, .17, .08, \overline{0}$	b	.54	
$Q(5)$	(σ) overall .33 (π) overall .33	b d	.31 .31	
$P(2)$	(σ) $\pm .\overline{33}, .17, 0$	d	.59	
$P(4)$	(σ) $\pm .20, .15, .10, .05, 0$	d	.39	
$P(6)$	(σ) overall .28	b	.27	
$P(8)$	(σ) overall .22	b	.21	
	$4d\delta, {}^3\Delta^{(0)} \rightarrow 2p\pi, {}^3\Pi^{(0)}$ ($\lambda = 4403$)			
$Q(2)$	(σ) $\pm 1.17, .\overline{67}, .33, .\overline{17}$ (π) $\pm\overline{1}.\overline{00}, .50$	q d	$\pm .67, .17$ 1.96	$\pm .33, .17, \overline{0}$ $\pm .\overline{33}, .17$
$Q(3)$	(σ) $\pm .83, .42, .59, .\overline{33}, .17, .\overline{08}$ (π) $\pm .\overline{75}, .50, .25$	d d	.84 1.47	$\pm 1.67, 1.25, 1.08, .67, .\overline{50}, .08$ $\pm\overline{1}.\overline{75}, 1.17, .68$
$Q(5)$	(σ) $\pm .54, .44, .37, .33, .27, .23, .17, .\overline{13}, .07, .\overline{03}$ (π) $\pm .\overline{50}, .40, .20, .10$	b d	.83 .96	$\pm 1.80, 1.50, 1.43, 1.13, 1.07, .77, .70, .40, .\overline{33}, .\overline{03}$ $\pm\overline{1}.\overline{86}, 1.45, 1.40, .73, .37$
$Q(6)$	(σ) overall .90 (π) overall .86	b d	.48 .79	overall 1.36 overall 1.43
$Q(8)$	(σ) overall .68 (π) overall .66	b d	.48 .68	overall 1.52 overall 1.55
$Q(10)$	(σ) overall .56 (π) overall .54	b d	.96 1.05	overall 1.62 overall 1.63
$Q(14)$	(σ) overall .47	b	.98	overall 2.34
$R(1)$	(σ) $\pm .\overline{83}, .67, .50$ (π) $\pm .17, \overline{0}$	d b	1.58 .30	$\pm .\overline{50}, 0$ $\pm .50, \overline{0}$

TABLE I. (*Continued*).

Line		Predicted, Case b'	Observed		Predicted, Case d'
$R(2)$	(σ)	$\pm .\overline{67}, .50, .33, .17, 0$	d	1.26	$\pm\overline{1}.\overline{83}, 1.17, .83, .50, .17$
$P(3)$	(σ)	$\pm\overline{1}.\overline{25}, 1.08, .67, .50, .08$	t	$\pm .73, 0$	$\pm .\overline{25}, .17, .08, 0$
	(π)	$\pm .85, .57, .28, \overline{0}$	t	$\pm .58, 0$	$\pm .17, .08, \overline{0}$
$P(4)$	(σ)	$\pm .\overline{90}, .80, .62, .52, .33, .23, .05$	b	1.37	$\pm\overline{1}.\overline{70}, 1.60, 1.15, 1.05, .60, .50, .05$
	(π)	$\pm .85, .57, .28, \overline{0}$	t	$\pm .25, 0$	$\pm 1.65, 1.10, .55, \overline{0}$
$P(5)$	(σ)	$\pm .\overline{70}, .63, .53, .47, .37, .30, .20, .13, .03$	d	1.30	$\pm .\overline{57}, .50, .43, .37, .30, .23, .17, .10, .03$
	(π)	$\pm .67, .50, .33, .17, \overline{0}$	b	.47	$\pm .53, .40, .27, .13, \overline{0}$
$P(7)$	(σ)	overall .97	d	1.01	overall 1.32
$P(9)$	(σ)	overall .73	d	.87	overall 1.53
$P(11)$	(σ)	overall .56	d	.69	overall 1.65
		$3d\delta,{}^3\Delta^{(0)}\rightarrow 2p\pi,{}^3\Pi^{(0)}$ ($\lambda=5733$)			
$Q(2)$	(σ)	$\pm 1.17, .\overline{67}, .33, .\overline{17}$	q	$\pm .70, .19$	$\pm .33, .17, \overline{0}$
	(π)	$\pm\overline{1}.\overline{00}, 50$	d	1.90	$\pm .\overline{33}, .17$
$Q(3)$	(σ)	$\pm .83, .59, .42, .\overline{33}, .17, .\overline{08}$	d	.89	$\pm 1.67, 1.25, 1.08, .67, .\overline{50}, .\overline{08}$
$Q(4)$	(σ)	$\pm .65, .50, .40, .35, .25, .\overline{20}, .10, .\overline{05}$	d	.60	$\pm .55, .50, .45, .40, .25, .20, .\overline{10}, .\overline{05}$
	(π)	$\pm .\overline{60}, .45, .30, .15$	d	.93	$\pm .\overline{60}, .45, .30, .15$
$Q(5)$	(σ)	$\pm .54, .44, .37\ .33\ .27, .23, .17, .\overline{13}, .07, .\overline{03}$	d	.77	$\pm 1.80, 1.50, 1.43, 1.13, 1.07, .77, .70, .40, .\overline{33}, .03$
$R(1)$	(σ)	$\pm .\overline{83}, .67, .50$	d	1.32	$\pm .\overline{50}, 0$
$R(2)$	(σ)	$\pm .\overline{67}, .50, .33, .17, 0$	d	.84	$\pm\overline{1}.\overline{83}, 1.17, .83, .50, .17$
$P(4)$	(π)	$\pm .85, .57, .28, \overline{0}$	d	.61	$\pm 1.65, 1.10, .55, \overline{0}$
		$4d\pi,{}^3\Pi^{(0)}\rightarrow 2p\pi,{}^3\Pi^{(0)}$ ($\lambda=4440$)			
$Q(2)$	(σ)	$\pm .\overline{17}$	d	.33	$\pm 1.50, .\overline{83}, .50, .17$
	(π)	$\overline{0}$	s		$\pm\overline{1}.\overline{33}, .67$
$Q(4)$	(σ)	$\pm .\overline{05}$	t	$\pm .24, 0$	$\pm 1.25, .95, .85, .65, .\overline{35}, .25, .\overline{05}$
	(π)	$\overline{0}$	d	1.12	$\pm\overline{1}.\overline{20}, .90, .60, .30$
$Q(10)$	(σ)	overall .02	b	.37	overall 2.36
$Q(12)$	(π)	overall .01	d	1.22	overall 2.26
$R(3)$	(σ)	$\pm .15, .12, .08, .\overline{05}, .02$	d	1.07	$\pm\overline{1}.\overline{15}, .88, .62, .45, .35, .18, .08$
	(π)	$\pm .10, .07, .03, \overline{0}$	b	.63	$\pm .80, .53, .27, \overline{0}$
$R(5)$	(σ)	$\pm .07, .06, .05, .\overline{03}, .02, .01, .00$	d	1.55	$\pm\overline{1}.\overline{12}, .94, .76, .69, .57, .51, .40, .33, .21, .14, .03$
	(π)	$\pm .03, .02, .01, \overline{0}$	b	.82	$\pm .90, .73, .54, .36, 1.8, .\overline{0}$

TABLE I. (*Continued*)

Line	Predicted, Case b'	Observed	Predicted, Case d'
$R(11)$	(σ) overall .03	d 1.61	overall 2.13
	(π) overall .02	b 1.63	overall 1.92
$R(15)$	(σ) overall .02	d 1.70	overall 2.09
$R(15)$	(σ) overall .02	d 1.77	overall 2.07
$P(3)$	(σ) $\pm .25, .17, .\overline{08}, 0$	d .39	$\pm 1.59, \overline{1}.\overline{42}, .83, .66, .08$
	(π) $\pm .17, .08, \overline{0}$	b .36	$\pm 1.50, .75, \overline{0}$
$P(5)$	(σ) $\pm .08, .05, .\overline{03}, .02$	d 1.32	$\pm 1.30, \overline{1}.\overline{23}, .98, .92, .67, .60, .35, .28, .03$
	(π) $\pm .07, .05, .\overline{03}, .02, 0$	b 1.06	$\pm 1.27, .95, .63, .32, \overline{0}$
$P(7)$	(σ) overall .07	t $\pm 1.04, 0$	overall 2.34
	(π) overall .07	b 1.22	overall 2.30
$P(9)$	(σ) overall .04	t $\pm .75, 0$	overall 2.18
	$3d\pi, {}^3\Pi^{(0)} \rightarrow 2p\pi, {}^3\Pi^{(0)}$ ($\lambda = 5887$)		
$Q(2)$	(σ) $\pm .\overline{17}$	d .32	$\pm 1.50, .\overline{83}, .50, .17$
	(π) 0	s	$\pm \overline{1}.\overline{33}, .67$
$Q(4)$	(σ) $\pm .\overline{05}$	b .47	$\pm 1.25, .95, .85, .65, .\overline{35}, .25, .\overline{05}$
	(π) 0	d .98	$\pm \overline{1}.\overline{20}, .90, .60, .30$
$R(3)$	(σ) $\pm .15, .12, .08, .\overline{05}, .02$	d .99	$\pm \overline{1}.\overline{15}, .88, .62, .45, .35, .18, .08$
	(π) $\pm .10, .07, .03, \overline{0}$	b .62	$\pm .80, .53, .27, \overline{0}$
$R(5)$	(σ) $\pm .07, .06, .05, .03, .02, .02, .\overline{01}, 0$	d 1.39	$\pm \overline{1}.\overline{12}, .94, .76, .69, .57, .51, .40, .33, .21, .14, .03$
	(π) $\pm .03, .02, .01, \overline{0}$	b .79	$\pm .90, .73, .54, .36, .18, \overline{0}$
$P(3)$	(σ) $\pm .25, .17, .\overline{08}, 0$	d .36	$\pm .159, \overline{1}.\overline{42}, .83, .66, .08$
	(π) $\pm .17, .08, \overline{0}$	b .34	$\pm 1.50, .75, \overline{0}$
	$3d\sigma, {}^3\Sigma^{(0)} \rightarrow 2p\pi, {}^3\Pi^{(0)}$ ($\lambda = 5954$)		
$Q(1)$	(σ) $\pm .50, \overline{0}$	t $\pm .47, 0$	$\pm 1.50, .\overline{50}$
	(π) $\pm .50$	d 1.00	$\pm \overline{1}.\overline{00}$
$Q(3)$	(σ) $\pm .25, .17, .\overline{08}, 0$	t $\pm .47, 0$	$\pm 1.83, 1.25, 1.08, .\overline{67}, .50, .\overline{08}$
	(π) $\pm .\overline{25}, .17, .08$	d 1.25	$\pm \overline{1}.\overline{76}, 1.17, .59$
$Q(5)$	(σ) $\pm .17, .13, .10, .\overline{07}, .03, 0$	t $\pm .35, 0$	$\pm 1.87, 1.50, 1.43, 1.13, .77, .70, .\overline{40}, .33, .\overline{03}$
	(π) $\pm .\overline{17}, .13, .10, .07, .03$	d 1.48	$\pm \overline{1}.\overline{83}, 1.47, 1.10, .73, .37$
$Q(7)$	(σ) overall .25	t $\pm .31, 0$	overall 3.78
	(π) overall .25	d 1.84	overall 3.50
$Q(9)$	(π) overall .20	d 2.10	ovrall 3.80
$Q(13)$	(σ) overall	t $\pm .28, 0$	overall 3.86
$P(2)$	(σ) $\pm .33, .17, 0$	d .70	$\pm 1.50, \overline{1}.\overline{17}, .17$
	(π) $\pm .17, \overline{0}$	b .37	$\pm 1.33, \overline{0}$

TABLE I. (*Continued*)

Line		Predicsted, Case b'	Observed		Predicated, Case d'
$P(4)$	(σ)	$\pm .\overline{20}, .15, .10, .05, \overline{0}$	d	1.19	$\pm 1.90, \overline{1}.\overline{80}, 1.28, 1.18, .67, .57, .05$
	(π)	$\pm .15, .10, .05, \overline{0}$	b	.92	$\pm 1.85, 1.23, .62, \overline{0}$
$R(2)$	(σ)	$.\overline{33}, .17, 0$	d	1.43	$\pm \overline{1}.\overline{67}, 1.17, .67, .33, .17$
	(π)	$\pm .33, .17, \overline{0}$	b	.86	$\pm 1.00, .50, \overline{0}$
$R(4)$	(σ)	$\pm .\overline{20}, .15, .10, .05, 0$	d	1.42	$\pm \overline{1}.\overline{85}, 1.45, 1.10, 1.00, .75, .65, .40, .30, .05$
		$4d\sigma,^3\Sigma^{(0)} \rightarrow 2p\pi,^3\Pi^{(0)}$ ($\lambda = 4458$)			
$Q(1)$	(σ)	$\pm .50, \overline{0}$	t	$\pm .52, 0$	$\pm \overline{1}.\overline{50}, .50$
	(π)	$\pm .\overline{50}$	d	1.00	$\pm \overline{1}.\overline{00}$
$Q(3)$	(σ)	$\pm .25, .17, .\overline{08}, 0$	t	$\pm .53, 0$	$\pm 1.83, 1.25, 1.08, .\overline{67}, .50, .\overline{08}$
	(π)	$\pm .\overline{25}, .17, .08$	d	1.35	$\overline{1}.\overline{75}, 1.17, .59$
$Q(5)$	(σ)	$\pm .\overline{17}, .13, .10, .\overline{07}. .03, 0$	t	$\pm .71, 0$	$\pm 1.87, 1.50, 1.43, 1.13, .77, .70, .\overline{40}, .33, .\overline{03}$
	(π)	$\pm .\overline{17}, .13, .10, .07, .03$	d	2.14	$\pm \overline{1}.\overline{83}, 1.47, 1.10, .73, .37$
$R(2)$	(σ)	$\pm .\overline{33}, .17, 0$	d	1.48	$\pm \overline{1}.\overline{67}, 1.17, .67, .33, .17$
	(π)	$\pm .33, .17, \overline{0}$	b	.92	$\pm 1.00, .50, \overline{0}$
$R(4)$	(σ)	$\pm .\overline{20}, .15, .10, .05, 0$	d	1.67	$\pm \overline{1}.\overline{85}, 1.45, 1.10, 1.00, .75, .65, .40, .30, .05$
	(π)	$\pm .20, .15, .10, .05, \overline{0}$	b	1.04	$\pm 1.40, 1.05, .70, .35, \overline{0}$
$R(8)$	(σ)	overall .22	d	1.67	overall 3.78
	(π)	overall .22	b	1.13	overall 3.33
$R(10)$	(σ)	overall .18	d	1.86	overall 3.82
	(π)	overall .18	b	1.21	overall 3.45
$P(2)$	(σ)	$\pm .\overline{33}, .17, 0$	d	.76	$\pm 1.50, \overline{1}.\overline{17}, .17$
	(π)	$\pm .17, \overline{0}$	b	.40	$\pm 1.33, \overline{0}$
		$4d\sigma,^3\Sigma^{(1)} \rightarrow 2p\pi,^3\Pi^{(1)}$ ($\lambda = 4479$)			
$Q(1)$	(π)	$\pm .\overline{50}$	d	1.03	$\pm \overline{1}.\overline{00}$
$Q(3)$	(π)	$\pm .\overline{25}, .17, .\overline{08}$	d	1.35	$\pm \overline{1}.\overline{75}, 1.17, .59$
$Q(5)$	(π)	$\pm .\overline{17}, .13, .10, .07, .03$	d	2.12	$\pm \overline{1}.\overline{83}, 1.47, 1.10, .73, .37$
$Q(7)$	(π)	overall .25	d	2.06	overall 3.50

As a summary of these observational results, Fig. 4 has been prepared to show at least qualitatively the magnetic field energy level patterns for some of those states in which uncoupling has been observed. The magnetic splitting of the $2p\pi,^3\Pi$ level has been assumed to follow case b' rigorously, as pointed out above. This made it possible to at least estimate, or in the case of resolved patterns, to determine definitely the energy of the levels of $4d\delta,^3\Delta$; $4d\pi,^3\Pi$; $4d\sigma,^3\Sigma$; and $3d\sigma,^3\Sigma$ in a magnetic field, wherever there were several observations involving the same rotational level. The numbers beside the levels or groups of levels are widths or separations in terms of $\Delta\nu_{\text{normal}}$.

SUMMARY

In summary, it may be said that Zeeman patterns in the ortho-helium bands involving levels of the $d\delta,^3\Delta$; $d\pi,^3\Pi$; and $d\sigma,^3\Sigma$ types have beenf ound to agree with theoretical predictions. The Zeeman effect in these levels offers a means of following the phenomenon of the uncoupling of the orbital angular momentum of the excited electron from the electric axis predicted and observed by previous investigators.

The author is greatly indebted for advice and assistance on this problem to Professor Robert S. Mulliken at whose suggestion it was undertaken, and to Professor George S. Monk for valuable technical assistance.

APPENDIX

Derivation of formulas (1) and (2) appearing in text

(1) *Energy of the case b′ singlet state in a magnetic field.* In terms of the vector model,[3] the vector representing the angular momentum of the excited electron, $l^*h/2\pi$, is thought of as being so rigidly bound to the molecular axis that the projection of l^* on this axis is a true quantum number, λ, corresponding to an angular momentum $\lambda h/2\pi$. This vector precesses with that representing the nuclear rotation, $Oh/2\pi$ (not a quantum number) about their quantized resultant $K^*h/2\pi$. If then this molecule is placed in a magnetic field of strength H, K^* will process about H and a magnetic energy will appear. This energy is written by Hund[8] as

$$\Delta E_{\text{mag}} = \overline{\mu_1 \underline{\lambda} \cdot \underline{H}}.$$

The average value of the scalar product of the vectors λ and H is obtained by finding the average contribution of λ to K^* and then the average value of the quantized projection of K^* on the direction of H (i.e., the magnetic quantum number M). Resolving λ into components perpendicular and parallel to K^*, it is easily seen that the average value of the perpendicular component is zero while the contribution of the parallel component is $\lambda \cos(\lambda, K^*)$. The projection of this quantity on the direction of H is, $\lambda \cos(\lambda, K^*) \cos(K^*, H)$. Hence

$$\Delta E_{\text{mag}} = \mu_1 H \lambda \cos(H, K^*) \cos(\lambda, K^*).$$

Now

$$\cos(H, K^*) = M/K^*, \quad \cos(\lambda, K^*) = \lambda/K^*,$$
$$K^{*2} = K(K+1).$$

Hence

$$\Delta E_{\text{mag}} = \mu_1 H M \lambda^2 / K(K+1). \tag{1}$$

(2) *Energy of a case d′ singlet state in a magnetic field.* In terms of the vector model, the orbital angular momentum of the excited electron, $l^*h/2\pi$, is thought of as being totally uncoupled from the molecular axis. The vector representing this angular momentum and that representing the rotational

energy of the nuclei, $R^*h/2\pi$, precess about their quantized resultant K^*. The energy of the molecule in a magnetic field may be then calculated very much as above.

$$\Delta E_{\text{mag}} = \mu_1 \overline{\underline{l}^* \cdot \underline{H}}$$

$$l_{\parallel}^* = l^* \cos (l^*, K^*)$$

$$\Delta E_{\text{mag}} = \mu_1 H l^* \cos (l^*, K^*) \cos (K^*, H)$$

$$\cos (l^*, K^*) = \frac{l^{*2} + K^{*2} - R^{*2}}{2l^*K^*}$$

$$\cos (K^*, H) = M/K^*$$

$$K^{*2} = K(K+1), \quad l^{*2} = l(l+1), \quad R^{*2} = R(R+1)$$

$$\Delta E_{\text{mag}} = \frac{\mu_1 HM}{2K(K+1)} [K(K-1) + l(l+1) - R(R+1)]. \qquad (2)$$

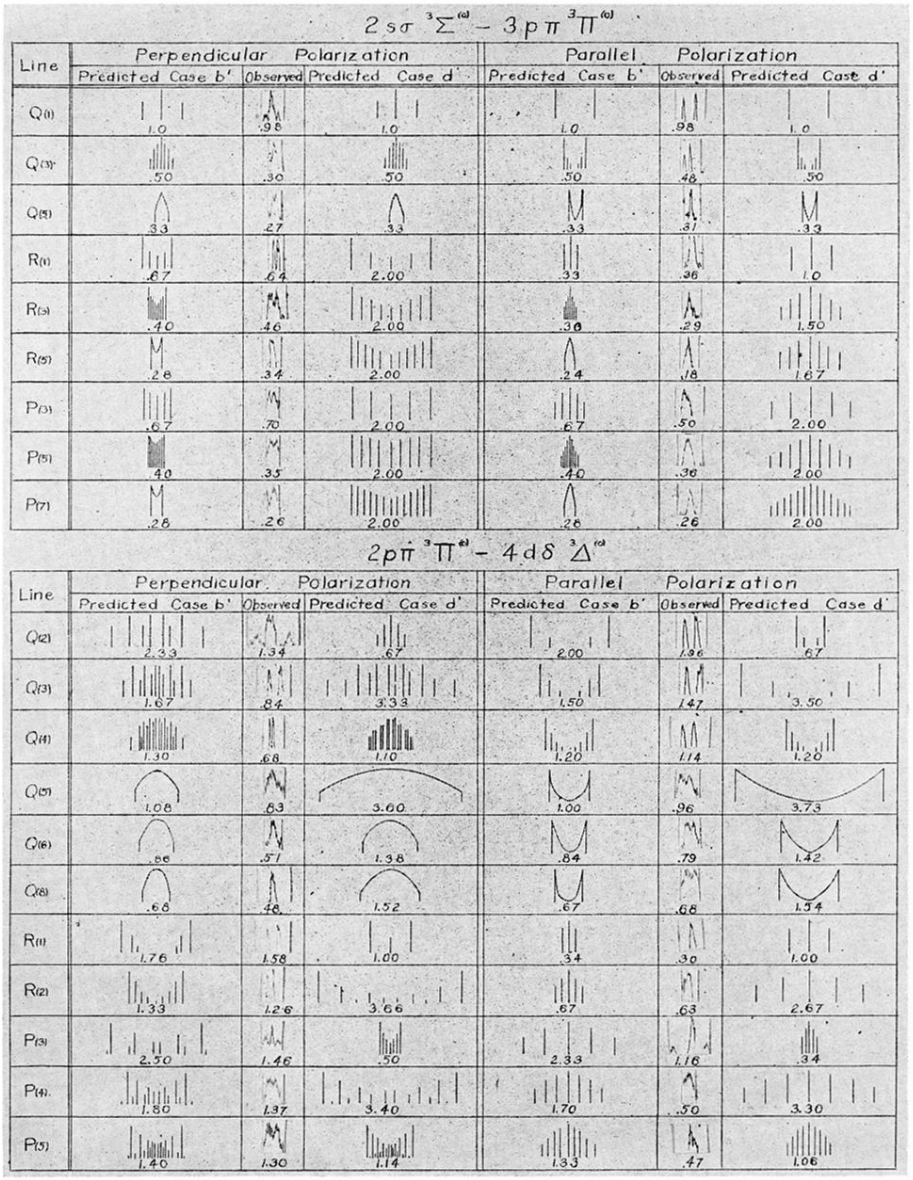

Fig. 1. Comparison of predicted Zeeman patterns and microphotometer traces of observed lines in bands in which there is little or no evidence of uncoupling phenomena The scale of the observed patterns is not uniform and is not the same as that of the predicted patterns.

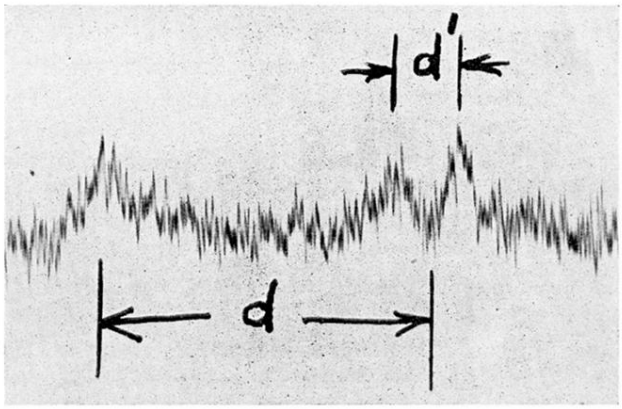

Fig. 2. Microphotometer trace of the anomalous line $Q(9)$ of $4p\pi,{}^3\Pi^{(0)}-2s\sigma,{}^3\Sigma^{(0)}$ in a magnetic field of 30,400 gauss. The perpendicular polarization is here reproduced but the trace in parallel polarization is very nearly identical. $d=6.61\ \mathrm{cm}^{-1}$, $d'=1.61\ \mathrm{cm}^{-1}$.

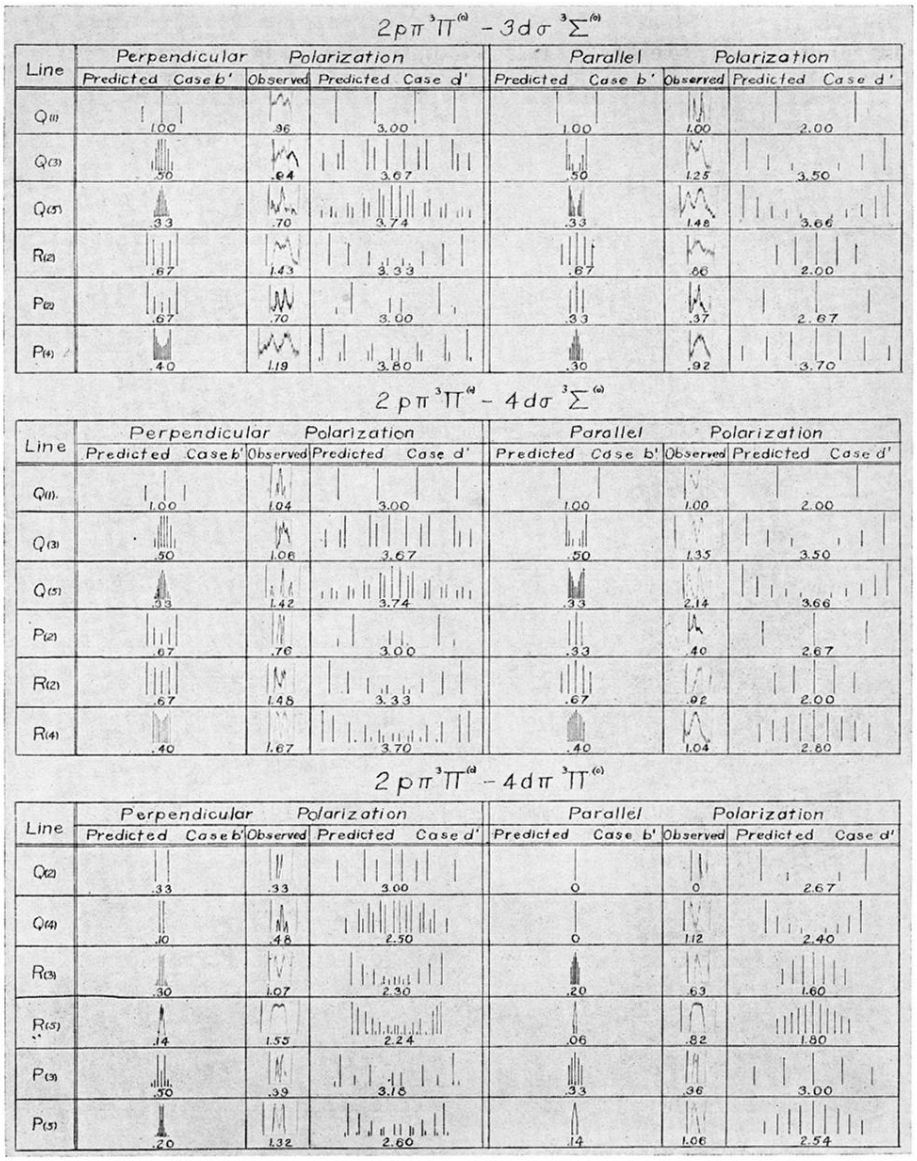

Fig. 3. Comparison of predicted and observed Zeeman patterns in bands which exhibit considerable evidence of uncoupling phenomena. The scales of the observed and predicted patterns are not the same.